Frontiers in Bioscience Landmark

Front. Biosci. (Landmark Ed) **2024**; 29(3): 108
https://doi.org/10.31083/j.fbl2903108

Original Research

Chitosan Membranes Stabilized with Varying Acyl Lengths Release Cis-2-Decenoic Acid and Bupivacaine at Controlled Rates and Inhibit Pathogenic Biofilm

Landon Reed Choi[1], Zoe Harrison[1], Emily C. Montgomery[1], Joshua R. Bush[1], Ezzuddin Abuhussein[1], Joel D. Bumgardner[1], Tomoko Fujiwara[2], Jessica Amber Jennings[1,*]

[1]Department of Biomedical Engineering, The University of Memphis, Memphis, TN 38111, USA
[2]Department of Chemistry, The University of Memphis, Memphis, TN 38152, USA
*Correspondence: jjnnings@memphis.edu (Jessica Amber Jennings)
Academic Editors: Piergiorgio Gentile and Viviana di Giacomo
Submitted: 13 July 2023 Revised: 14 December 2023 Accepted: 5 January 2024 Published: 18 March 2024

Abstract

Background: Adherence of complex bacterial biofilm communities to burned tissue creates a challenge for treatment, with infection causing 51% of burn victim deaths. This study evaluated the release of therapeutics from wound care biomaterials and their antimicrobial activity against pathogens *Staphylococcus aureus*, *Acinetobacter baumannii*, and *Pseudomonas aeruginosa*. **Methods**: Electrospun chitosan membranes (ESCMs) were fabricated and acylated with chain lengths ranging from 6–10 carbons then loaded with 0.15 mg of anti-biofilm agent, cis-2-decenoic acid (C2DA), and 0.5 mg of local anesthetic, bupivacaine. **Results**: Combinations of therapeutics released from modified ESCMs at a cumulative amount of 45–70% of bupivacaine and less than 20% of C2DA. Results from bacterial studies suggest that this combination reduced biofilm 10-fold for *S. aureus*, 2-fold for *Acinetobacter baumannii*, and 2–3-fold for *Pseudomonas aeruginosa* by 24 hours. Additionally, dual loaded groups reduced planktonic *Staphylococcus aureus* ~4-fold by 24 hours as well as *Acinetobacter baumannii* ~3-fold by 48 hours. **Conclusions**: The combination of therapeutics used has a significant role in biofilm prevention for selected strains via direct contact or diffusion in aqueous solutions.

Keywords: biofilm; infection; bupivacaine; C2DA; electrospinning; chitosan; biomaterial; anhydride; drug delivery

1. Introduction

Burn injury is a common global threat that causes complex wounds that may affect the whole body. According to the World Health Organization (WHO), it is estimated that 11 million burn injuries occur worldwide, accompanied by 180,000 deaths a year [1]. For individuals with moderate to severe burns, challenges such as infection, inflammatory/immune response, metabolic changes, and distributive shock are all factors that can lead to multiple organ failure [2]. This is especially the case for individuals in severe conditions and/or combat settings where delayed care could result in a loss of viable tissue and increase chances of obtaining a life-threatening infection. Infections with multi-drug resistant biofilms are especially difficult to treat as they present challenges for post-burn therapeutic care. Biofilm refers to a complex community of adherent bacteria that consist of single or multiple bacterial strains, that attaches to a surface while colonizing within a matter of 2–3 days [3,4]. Up to 80% of human bacterial infections are biofilm associated; such infections are most frequently caused by *Staphylococcus epidermidis*, *Pseudomonas aeruginosa*, *Staphylococcus aureus*, and *Escherichia coli* [5].

Mechanisms of biofilm tolerance include mechanical protection due to encasement in extracellular polymeric substance (EPS) as well as protection from antibiotic clearance via metabolically dormant persister cells [6]. Current treatments for burns include topical antimicrobial therapies such as silver sulfadiazine (Silvadene®) or mafenide (Sulfamylon®) cream [7,8] followed by the application of wound dressings. Although silver sulfadiazine dressings (SSD) are used commonly for second degree burns, they have been shown to potentially impair healing by exerting toxic effects on keratinocytes and fibroblasts [9].

Bacteria within biofilm release intrinsic signaling molecules, termed diffusible signal factors (DSF), to detach from the surface and allow for biofilm colonization throughout other areas of the body [10]. This cell-to-cell communication is known as quorum sensing, and it is performed by biofilm to assess and address the microenvironment it resides in [11]. We investigated cis-2-decenoic acid (C2DA), a short chain fatty acid that acts as a DSF involved with the regulation of biofilm growth, and virulence that can be used to disperse and inhibit biofilm formation [12–14]. Results from previous studies on the antimicrobial effects of C2DA show that it can prevent infection when acting alone and synergistically with other antibiotics [14,15]. In addition, the cis conformation contributes to membrane permeability, allowing the passage of small molecule antibiotics into the cell [14].

Local anesthetics (LA) have long been used as a therapeutic strategy for post-burn care in the form of topical sprays or creams, due to their pain numbing effects and their lack of interference with the healing process [16]. Additional benefits of using LAs include increasing blood perfusion to pre-burn levels [17], modification of the inflammatory response [18] to calm inflammation, and reducing edemas that contribute to the conversion of burn wounds to deeper layers of tissue. An additional benefit from LAs, such as bupivacaine, is its slow onset and long-lasting effects [19]. Similar to C2DA, local anesthetics such as bupivacaine are hydrophobic, making these molecules difficult to deliver.

Chitosan is extensively researched due to its abundant supply, versatility, biocompatibility, and biodegradability that facilitate its fabrication into local antibiotic delivery systems [20]. The medical potential behind chitosan is ever-growing as it can be fabricated into hydrogels, chitosan sponge delivery systems [21], magnetic chitosan nanoparticles for targeted drug delivery [22], coatings for musculoskeletal implant fixation hardware, injectable chitosan paste for traumatic injuries [23], and electrospun chitosan membranes (ESCM) [24,25]. Electrospinning is an inexpensive and reliable technique that entails dissolving a polymer and charging it to extrude the volatile solution onto a grounded plate where a multi-layered membrane is fabricated via nano-scale fiber collection. Previous work has shown chitosan nanofibrous membranes as well suited for tissue healing and drug delivery applications due to their increased surface area, high degree of biocompatibility and biodegradability, and ability to mimic the extracellular matrix [26–31]. Preliminary evaluations of ESCM have revealed unique properties that make them particularly suited for delivering anesthetics, fatty acids, and antimicrobials [32]. Furthermore, Chitosan nanofibers have been studied for their applications in tissue regeneration but are limited in that aspect due to their hydrophilic properties which lead to swelling, and degeneration of the fibers. Acylating the membranes with carbon chains makes the material hydrophilic and prevents swelling from happening [33]. As-spun membranes are modified via acylation using fatty acids of different chain lengths to protect from swelling and dissolution of membrane fibers in aqueous solutions at low pH [32]. Modification via acylation surrounds the core chitosan nanofiber with a hydrophobic surface and minimizes adherence of the fibers to wounded tissue, which is ideal for patient care during dressing changes. Prior research has gone into evaluating modified ESCM with short chain fatty acids, with success of extended release of hydrophobic therapeutics [24,25]. Preliminary studies assessed the cytocompatibility and release profile of therapeutics from ESCMs, and concluded that a concentration of 0.15 mg of C2DA and 0.5 mg of bupivacaine per 10 mm diameter ESCM is cytocompatible and allow for the controlled release of the drugs [25].

Electrospun chitosan membranes tailored with acyl lengths ranging from 6–10 carbons by reaction of fatty acid anhydride and loaded with both bupivacaine and C2DA may serve to (1) act as a physical barrier from microbial contamination, (2) release antimicrobial local anesthetic to reduce pain and modify the inflammatory response, (3) release natural antimicrobial fatty acids that prevent biofilm contamination, and (4) prolong delivery of these hydrophobic therapeutics for an extended period. These loaded membranes may be used as wound dressings for soft tissue wounds following 2nd and 3rd degree burns for prolonged prevention of infection and management of pain. In this study, we sought to determine release profiles of therapeutics from chitosan membranes and their ability to prevent *S. aureus* (UAMS-1; ATCC 21121), *A. baumannii* (BAA; 1710) and *P. aeruginosa* (PA; ATCC 27317) growth and biofilm formation.

2. Methods and Materials

2.1 Preparation of Electrospun Chitosan Materials

Membranes were electrospun using a 311.5 kDa chitosan (ChitoLytic, Ajax, Ontario, Canada) with an 86.5%-degree deacetylation. Chitosan was dissolved overnight at 5.5% (w/v) , of 70% (v/v) trifluoroacetic acid & 30% (v/v) dichloromethane. The solution was vortexed then centrifuged to remove any undissolved chitosan particulates. Afterward, the solution was transferred to a 10 mL syringe and electrospun into 15 mm diameters and ~0.7 mm (>10 mL spinning solution) thick membranes as described by Wu *et al*. [32]. Briefly, chitosan was dissolved in TFA/DCM solution and was ejected from a 20-gauge needle with a flow rate of 0.015–0.03 mL/min and at 14–26 kV. Fibers were collected on a non-stick aluminum foil 25 cm away from the needle and attached to a grounded metal wheel (18 cm in diameter) rotating at 8.4 RPM by an AC motor to ensure even and random distribution. The temperature and humidity were controlled at 25 °C and 50%, respectively.

Celox gauze (Medtrade Products Ltd., UK) is available commercially for purchase, and is made of granular chitosan. Celox gauze is typically used as a hemostatic agent which interacts with red blood cells to stop bleeding. It serves as the standard-of-care control in this study.

2.2 Anhydride Treatment

Discs 10 mm in diameter were punched out and modified using hexanoic (HA), octanoic (OA), or decanoic (DA) fatty acid anhydrides [24,32]. Chitosan was reacted with the anhydrides in pyridine for 1.5 hours then rinsed with acetone, 70% ethanol, and deionized water at room temperature (25 °C). After membranes have undergone the anhydride treatment, membranes are lyophilized (FreeZone 2.5, Kansas, MO, USA) for 24 hours. After treatment, samples are loaded with 5.071 µL/mL of C2DA and/or 16.67 mg/mL of bupivacaine via ethanol evaporation. These concentrations result in 0.15 mg of C2DA and/or 0.5 mg of

bupivacaine. One half of each specimen is used for characterization via elution/bacterial analysis and the other half of each specimen was used for quantifying loading.

2.3 Scanning Electron Microscopy

Treated and untreated membranes were imaged with Scanning Electron Microscopy (SEM) (Nova NanoSEM650, FEI Co., Hillsboro, OR, USA) to characterize fibers on the surface of the ESCMs. To prepare the SEM samples, membranes were placed on flat metal stubs to later be sputter coated (EMS Quorum/Q 150T ES plus, Quorum, UK) with a 5.2 nm gold-palladium coating of argon and nitrogen. Images were taken through a backscattered electron detector (BSE), with an accelerating voltage of 20 kV and a working distance of 5.1 mm. After images were taken via SEM, fiber width was recorded and compared to scale bars from the same SEM image to accurately measure the width. Three SEM images were analyzed for each group and 20 fibers from each SEM image were measured. Fiber measurements were done via ImageJ software (Version 1.53r, NIH, Bethesda, MD, USA).

2.4 Fourier Transform Infrared Spectroscopy

Treated membranes were observed using PerkinElmer Frontier FT-IR spectrometer (Waltham, MA), with a diamond crystal, in Attenuated Total Reflectance (ATR) mode to analyze the bonds on the surface of ESCMs, and to verify the success of fabrication and treatment via ester bonds, decreased presence of chitosan salts, and an increase in carbon chain. The analysis was done at room temperature (25 °C), at a spectral resolution of 8 cm^{-1}, and a range of 500 cm^{-1} to 4000 cm^{-1}.

2.5 Water Contact Angle

Water contact angle was performed to determine changes in ESCM hydrophobicity following each anhydride treatment (HA, OA, and DA). Treated membranes were placed on a VCA Optima (AST Products, Billerica, MA, USA) stage where a water droplet (5 µL) was slowly dropped on top of the sample and left for 5 minutes (n = 3 per treatment group). Contact angle for each sample was determined using VCA OptimaXE software (AST Products, Inc., Billerica, MA, USA).

2.6 X-ray Photoelectron Spectroscopy

X-ray Photoelectron Spectroscopy (XPS) was utilized to look at the surface of the samples for the percentage of elements associated with treated groups. In addition to the elemental analysis, XPS results were used to calculate the Degree of Substitution (DOS) [32]. Analysis of the samples was performed using a ThermoScientific K-Alpha XPS system equipped with a monochromatic X-ray source at 1486.6 eV, corresponding to the Al Ka line. The X-ray power of 75 W at 12 kV was used for all experiments with a spot size of 400 mm^2. The base pressure of the K-Alpha instrument was at 7.5 $\times$ 10^{-10} mBar. The instrument was calibrated to give a binding energy of 84.0 eV for Au 4f7/2 and 284.8 for the C1s line of adventitious (aliphatic) carbon present on the nonsputtered samples. Photoelectrons were collected from a takeoff angle of 900 relative to the sample surface. A series of XPS spectra were acquired in the Constant Analyzer Energy mode. The survey spectra were collected at a pass energy of 200 eV and an energy step size of 1.0 eV, while the high resolution (HR) core level spectra of C1s, O1s, etc. were taken at a 40 eV pass energy, an energy step size of 0.1 eV, and using an average of 40 scans (n = 2). The XPS data acquisition was performed using the Avantage v5.995 software (Thermo Fisher Scientific Inc., Waltham, MA, USA) provided with the instrument. Degree of substitution was calculated according to Eqn. 1:

$$A\%C : A\%N = \left(\frac{6+px}{1}\right) * 0.865 + \left(\frac{8+px}{1}\right) * 0.135 \quad (1)$$

where *A%C* is atomic percentage of carbon, *A%N* is atomic percentage of nitrogen, *p* is the number of carbons in the chain, and *x* is the degree of substitution.

2.7 Elution Profile

Loaded half samples (samples with a diameter of 10 mm, cut in half) (n = 5 per group) were weighed and placed in sterile phosphate buffered saline (PBS) with 10% bovine growth serum (Hyclone, Logan, Utah), eluates were collected by complete solution change at time points of 3, 6, 9, 12, 24, 36, 48, 60, and 72 h. The other half of each sample was saved for a single time point analysis following a 100% ethanol wash. The concentration of C2DA and bupivacaine in the eluates was measured with high performance liquid chromatography (HPLC) using a ThermoScientific Dionex Ultimate 3000 Series HPLC system and a BDS Hypersil reversed-phase C18 column (particle size of 5 µm) (250 $\times$ 4.6 mm) (run time = 7 min, injection volume = 10 µL, wavelength = 197 nm, dilution factor = 1.0). All eluate concentrations were normalized to standard curves with known concentrations of C2DA and bupivacaine.

2.8 Antimicrobial Activity

Loaded and unloaded samples (n = 4) were placed in 24 well plates and inoculated with 0.5 mL tryptic soy broth (TSB) containing 10^6 colony forming units (CFU) of *S. aureus* (UAMS-1; ATCC 21121), *A. baumannii* (BAA; 1710) or *P. aeruginosa* (PA; ATCC 27317). After incubating at 37 °C for 24 or 48 hours, membranes were removed from wells, rinsed twice with sterile PBS (pH = 7.4), and sonicated for 5 min at 40 kHz (Fisher Scientific Ultrasonic Bath, 9.5 L) to remove biofilm-associated bacteria. Quantification of biofilm was determined using BacTiter-Glo® Microbial Cell Viability Assay (Promega). To quantify the presence of viable planktonic bacteria, supernatants from

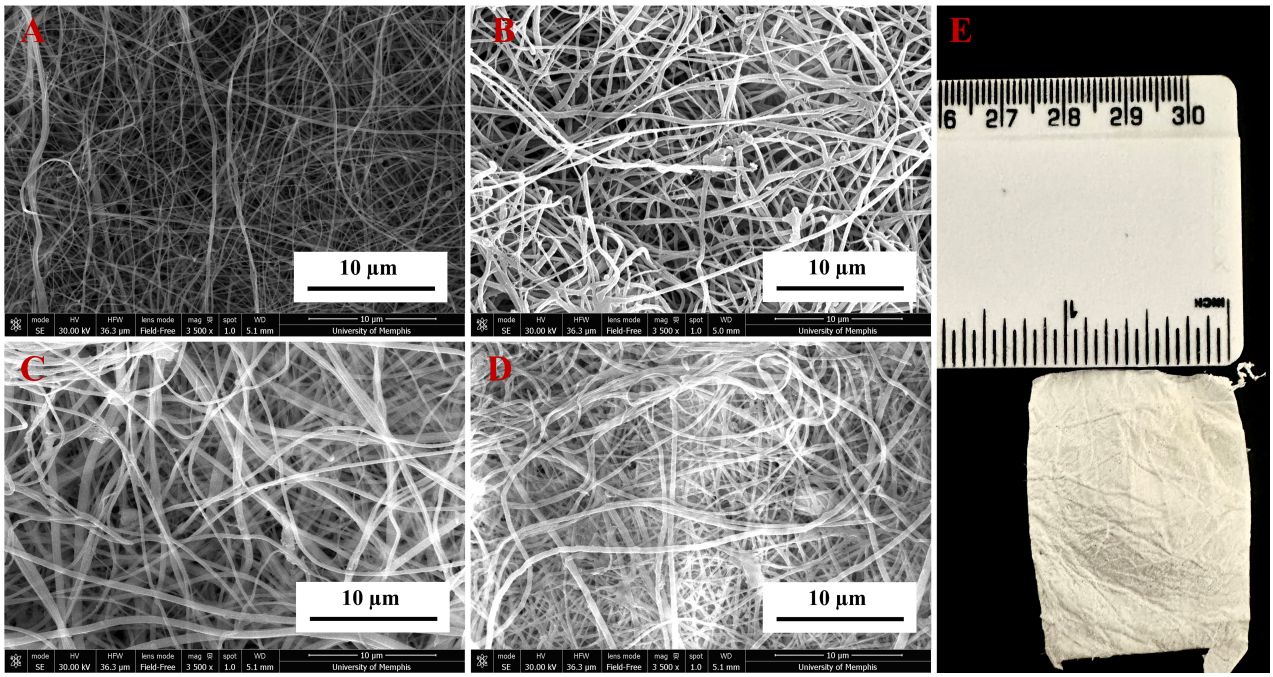

Fig. 1. SEM images of unmodified and modified electrospun chitosan membranes. (A) unmodified, (B) modified with Hexanoic anhydride, (C) modified with Octanoic anhydride, (D) modified with Decanoic anhydride, (E) macroscopic image of unmodified electrospun membrane. SEM, scanning electron microscopy.

Table 1. Average fiber diameter of unmodified electrospun chitosan membrane (ESCM), and ESCM modified with various anhydrides. Statistical differences were tested against the unmodified control (n = 60).

Treatment	Average diameter (µm)	Statistical difference
ESCM (control)	0.469 ± 0.184	Not applicable; control
Hexanoic	0.432 ± 0.199	No difference (p = 0.592)
Octanoic	0.422 ± 0.195	No difference (p = 0.399)
Decanoic	0.435 ± 0.199	No difference (p = 0.658)

wells containing membranes and bacteria were removed after 24- or 48-hours exposure to membranes and added to a new 96 well plate, then combined with BacTiter-Glo®. Biofilm growth on tissue culture plastic for wells containing membranes was further analyzed to determine biofilm formation at sites distant from membranes. After membranes and supernatants were removed, wells were rinsed with PBS (2 times) and attached biofilm was quantified using BacTiter-Glo®. Results were normalized as a percent viability versus bacterial cells grown in untreated wells.

2.9 Statistical Analysis

Statistical analysis was performed using GraphPad Prism 9 software (GraphPad Software Incorporation, La Jolla, CA, USA) and Xrealstats (Add-in) through Excel. Data was assessed first by performing Shapiro-Wilk normality test, followed by Brown-Forsythe equal variance test. If both passed, data was further analyzed with a one-way analysis of variance (ANOVA) followed by Holm-Sidak's post-hoc analysis to detect significant between experimental groups (α = 0.05). If normality and equal variance were not passed, data was analyzed using Kruskal-Wallis ANOVA on ranks (α = 0.05), followed by Tukey post-hoc test or Dunn. Comparisons against control groups were performed with one-way ANOVA followed up with Dunnett C.

3. Results

3.1 Scanning Electron Microscopy

SEM images of the different anhydride treatments confirmed consistent fiber diameter with minimal swelling between the different treatments and control (ESCM) (Fig. 1), resulting in no significant differences between fiber diameters (Table 1). Forty fibers from each sample were measured using DiameterJ and the fiber diameters are reported in the histogram in Fig. 2.

3.2 Fourier Transform Infrared Spectroscopy

For the untreated membranes, characteristic peaks were observed at 720–840, 1790, 1670, 2300–3600, 1100 and 1200 cm^{-1} correspond to C-F stretching, C=O stretching, C=O making chitosan salt, broad O-H stretching, and large peaks caused from TFA. For the treated membranes, characteristic peaks were observed at 1742, ~3460 and ~3290, 1650, 1545, and 2900 cm^{-1} corresponding to C=O of ester, N-H stretching of amine (NH_2), C=O of amide,

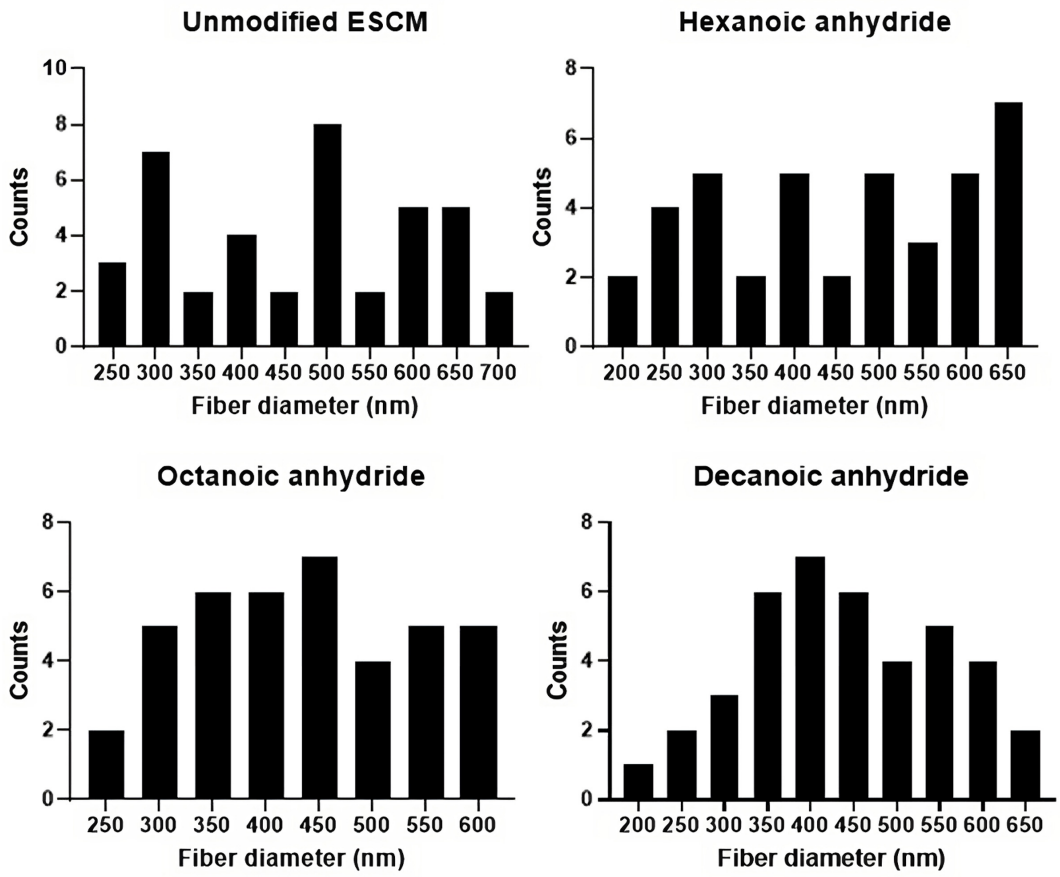

Fig. 2. Fiber diameter distribution of unmodified ESCM, and ESCM modified with various anhydrides (n = 40).

Table 2. The degree of substitution of ESCM after different anhydride modifications.

Treatments	Hexanoic anhydride	Octanoic anhydride	Decanoic anhydride
Degree of substitution (%)	1.51 ± 0.14	1.25 ± 0.39	1.13 ± 0.09

and N-H bend of chitosan amide, and acyl carbon chains at the surface of the membrane. All TFA peaks were absent or drastically decreased (Fig. 3).

3.3 Water Contact Angle

Each water drop stayed fixed on treated membranes for 5 minutes and all treated membranes exhibited hydrophobic properties (Fig. 4).

3.4 X-Ray Photoelectron Spectroscopy

XPS showed an increase in carbon detected starting with untreated through decanoic treated groups at binding energy 277–292 eV. Fig. 5 shows the XPS spectra for electrospun chitosan and the decanoic treated group. The various anhydride treatments lead to an increased C:N ratio which was then used to calculate the degree of substitution (DOS) (Table 2) using Eqn. 1. This increase in the C:N ratio resulted in a decrease in DOS, with all values being less than 2.

3.5 Bupivacaine Elution Profile

Results showed a high burst release of bupivacaine from the controls with chitosan sponge eluting no more by 36 hours and gauze eluting out to the end of the 3-days (Fig. 6). Experimental groups show a burst release within the first 3 hours followed by tapering concentrations throughout the 3-day elution. Octanoic anhydride treated membranes exhibited the highest burst release of bupivacaine from the experimental groups, followed by release of lower concentrations over the course of 3 days. Cumulative release showed significant differences between control groups vs. hexanoic and decanoic treated groups, while no significant differences were observed for octanoic group. Control groups released loading concentration within the first day, while all experimental groups released approximately 45% of the payload or more by the end of the 3 days.

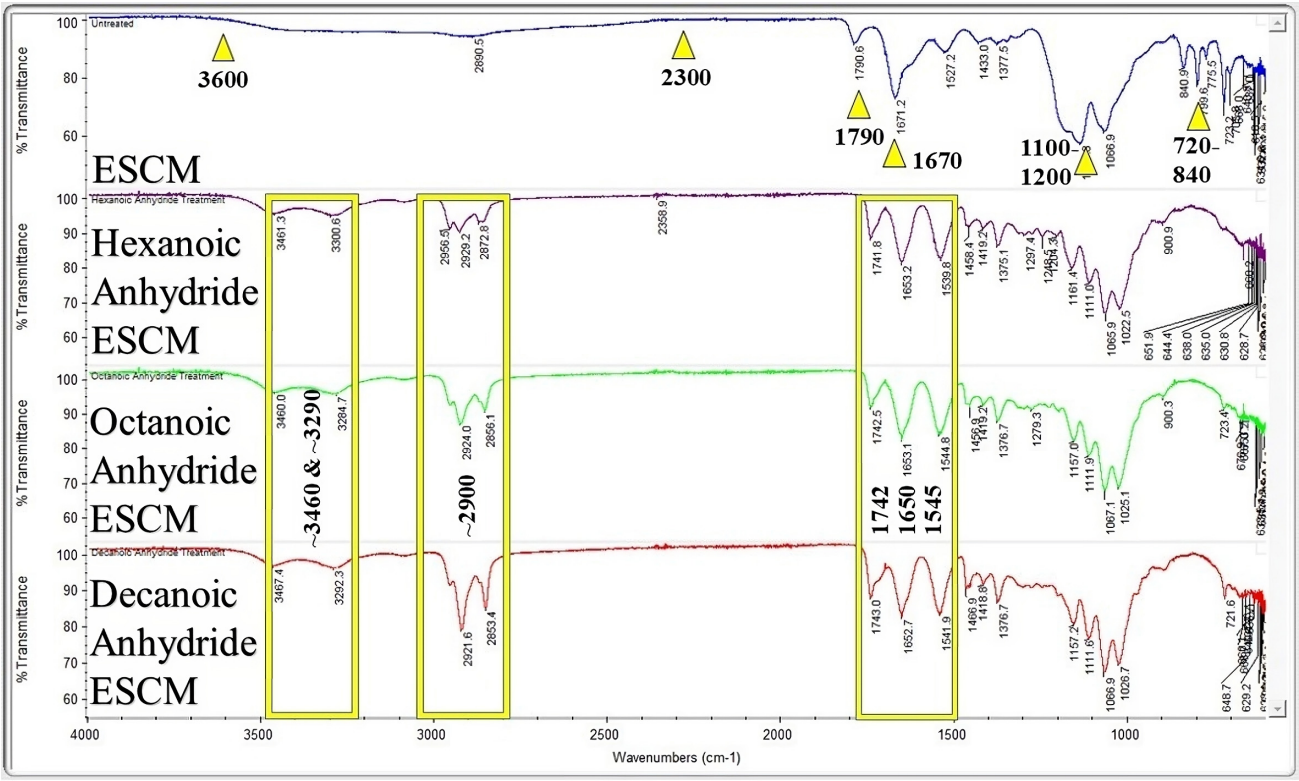

Fig. 3. Fourier transform infrared spectroscopy (FTIR) analysis of the as-spun ESCM and the ESCMs with the varying anhydride treatment. The arrows are for emphasis on the prior discussed peaks, boxes are for grouping peaks between spectra.

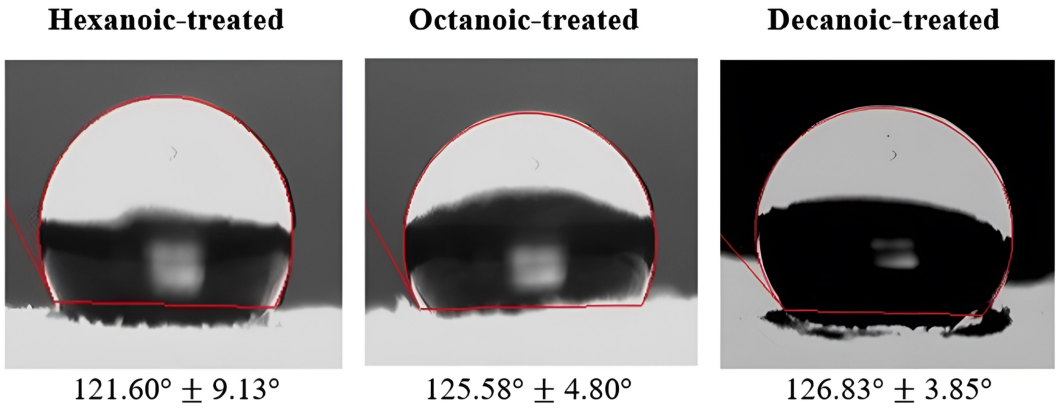

Fig. 4. Contact angle images of anhydride treated ESCMs and their corresponding averaged left/right angles ± the standard deviation (n = 3).

3.6 C2DA Elution Profile

Results from the 3-day release (Fig. 7) showed all samples start with a burst release within the first 3 hours then tapering concentrations at 6 hours. By 24 hours, only the experimental groups released C2DA. C2DA release was not detected for any groups within the 12-hour timepoint or after 24 hours. There was a significant difference in the release of C2DA between octanoic ESCM and chitosan sponge vs. hexanoic ESCM. Additionally, all samples only released less than 20% of the C2DA payload.

3.7 Antimicrobial Activity

3.7.1 *S. aureus*

Results from the *S. aureus* planktonic analysis showed all groups had significantly lower growth compared to bacteria control within the first 24 hours (Fig. 8). By the second day, only groups loaded with both C2DA, and bupivacaine had significantly lower planktonic growth compared to control. As for the biofilm associated on the wells of the plates, control groups were similar to untreated bacteria, while experimental groups show high variability within the

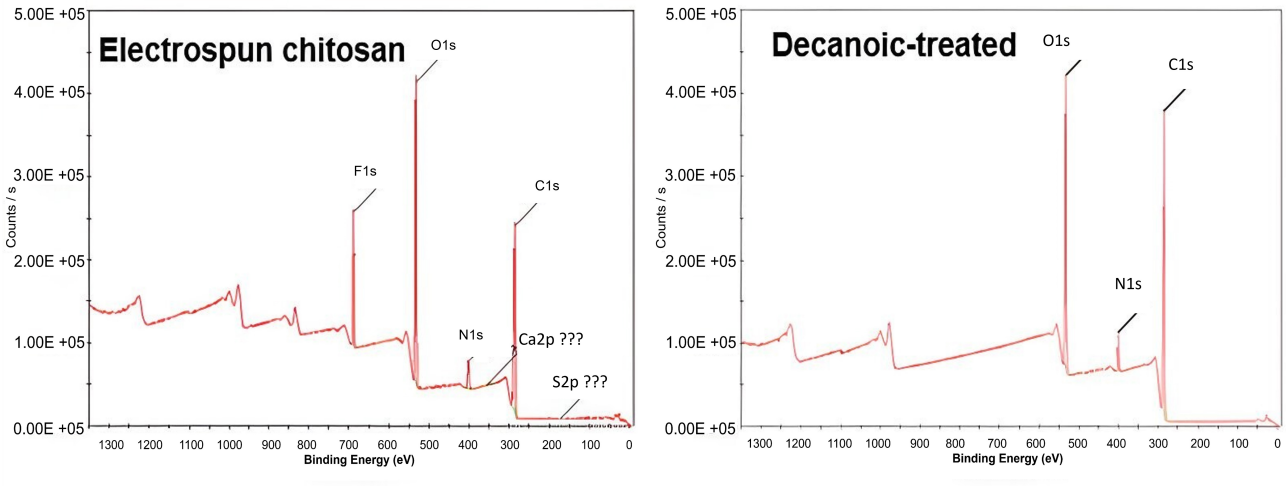

Fig. 5. X-ray photoelectron spectroscopy (XPS) results for electrospun chitosan and the decanoic anhydride treated group.

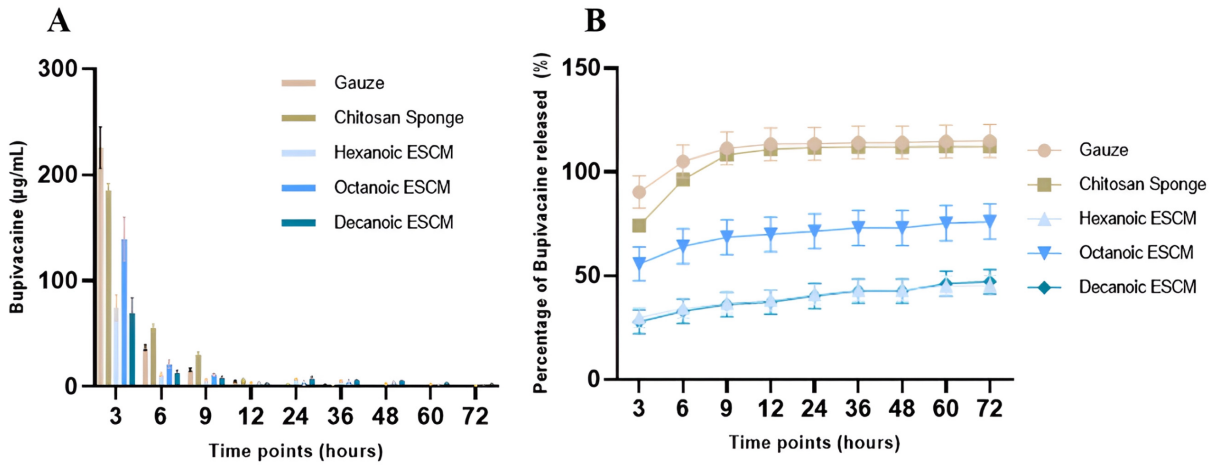

Fig. 6. Bupivacaine elution profile. (A) Hourly release of Bupivacaine over the course of 3 days. (B) Cumulative release of bupivacaine over the course of 3 days. Values plotted are the means ± the standard deviation. Significant differences were determined by Kruskal-Wallis ANOVA on ranks, followed by Dunn test (n = 5).

first 24 hours. Significant differences over the control were detected for decanoic + C2DA by 24 hours, by 48 hours, all groups showed similar growth rates to that of the bacteria control outside from gauze. Biofilm associated with membranes showed both chitosan sponge at 24 hours and 48 hours significantly higher than the rest of the groups. Additionally, all the ESCM resulted in the least amount of *S. aureus* biofilm viability at both 24 and 48 hours. Images of the samples' surfaces were taken via SEM showing more colonies present on the surface of the samples within the first 24 hours (Fig. 9).

3.7.2 *A. baumannii*

Results from the *A. baumannii* planktonic analysis showed all groups to be similar to that of the bacteria control at 24 hours (Fig. 10). At 48 hours, the groups loaded with the combination of C2DA and bupivacaine were the only groups significantly lower to the bacteria control. This was also the case for the biofilm plate analysis at 24 hours, where the combination of therapeutics inhibits the most growth compared to the other loaded or unloaded groups. By the end of 48 hours, all groups were similar to that of the bacteria control. The biofilm associated with the membranes showed that the chitosan sponge and gauze was significantly higher than all the other groups within the first 24 hours. Within 48 hours, Decanoic ESCM loaded with bupivacaine showed a significant decrease in viability compared with gauze and Decanoic ESCM. The chitosan sponge loaded with C2DA and bupivacaine showed a significant decrease in viability compared with gauze, De-

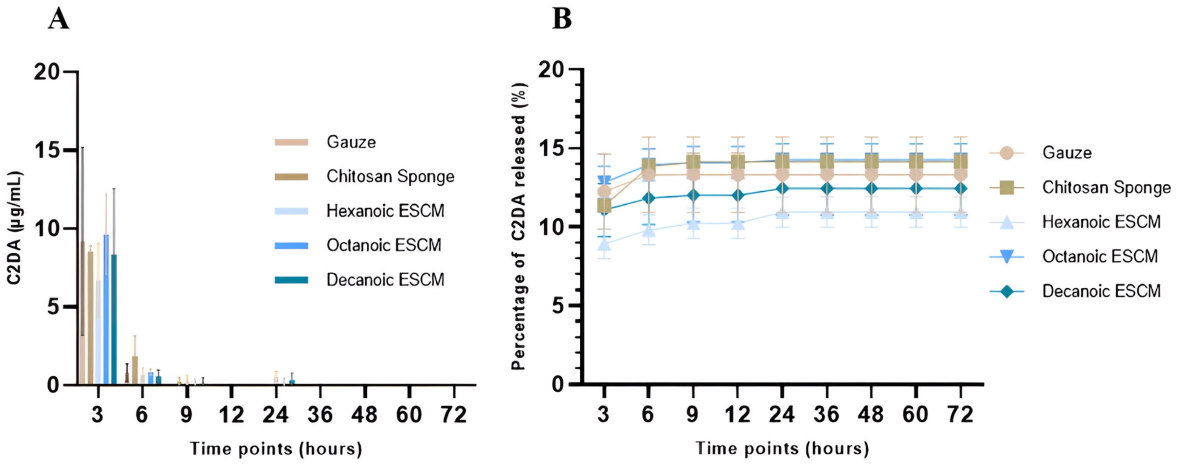

Fig. 7. Cis-2-decenoic acid (C2DA) elution profile. (A) hourly release of C2DA over the course of 3 days and (B) cumulative release of C2DA over the course of 3 days Values plotted are the means ± the standard deviation. Significant differences were determined by Kruskal-Wallis ANOVA on ranks, followed by Dunn test (n = 5).

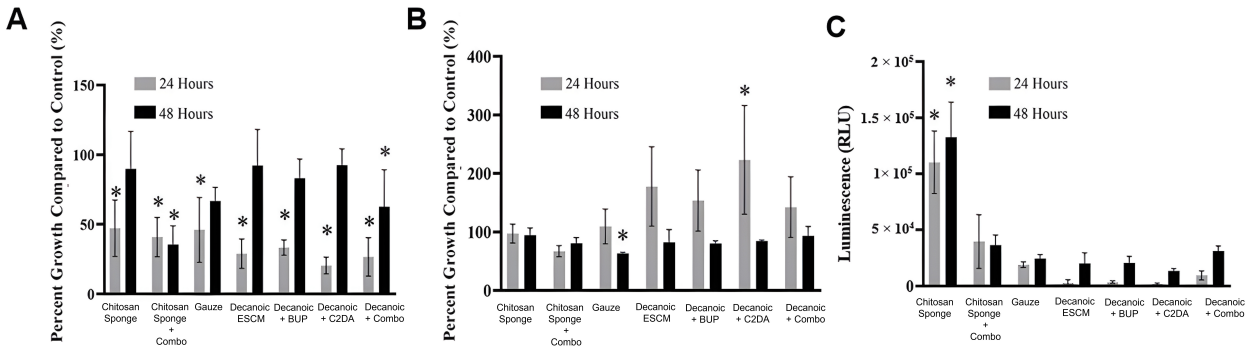

Fig. 8. *S. aureus* viability at 24 and 48 hours. (A) Planktonic viability, (B) biofilm found in the wells, and (C) biofilm found on samples. Values plotted are the means ± the standard deviation. Significant differences against bacteria control are represented by asterisks (*) as shown above ($p < 0.05$). Significant differences were determined by one-way ANOVA, followed by Dunnett C for figures with controls and Kruskal-Wallis ANOVA on ranks, followed by Tukey post-hoc test for figures with no controls (n = 5). BUP, Bupivacaine.

canoic ESCM, and Decanoic loaded with C2DA. Images of the sample's surface were taken via SEM showing continual growth at 24 hours, as seen with the biofilm growth on the membranes (Fig. 11).

3.7.3 *P. aeruginosa*

P. aeruginosa planktonic analysis for 24 hours showed all groups having growth similar to that of the control. By 48 hours, the chitosan sponge had significantly higher growth than the control (Fig. 12). Biofilm plates were later analyzed and results for 24 and 48 hours showed similar results to the bacteria control. Biofilm growth on the plates showed signs of decreased growth by the end of the 48 hours. Lastly the samples were analyzed for potential biofilm, results from the 24-hour analysis showed significant differences for chitosan sponge and chitosan sponge loaded with C2DA and bupivacaine, showing higher growth compared with Decanoic ESCM loaded with C2DA and Decanoic ESCM loaded with C2DA and bupivacaine. In addition to the 24-hour analysis, significantly higher growth was seen for gauze in comparison with Decanoic ESCM loaded with C2DA. The 48-hour analysis showed significantly higher growth for Decanoic loaded with C2DA against all other groups besides Decanoic ESCM and Decanoic loaded with C2DA and bupivacaine. Images of the samples' surfaces taken via SEM showed high growth within the first 24 hours as well as biofilm formation (Fig. 13).

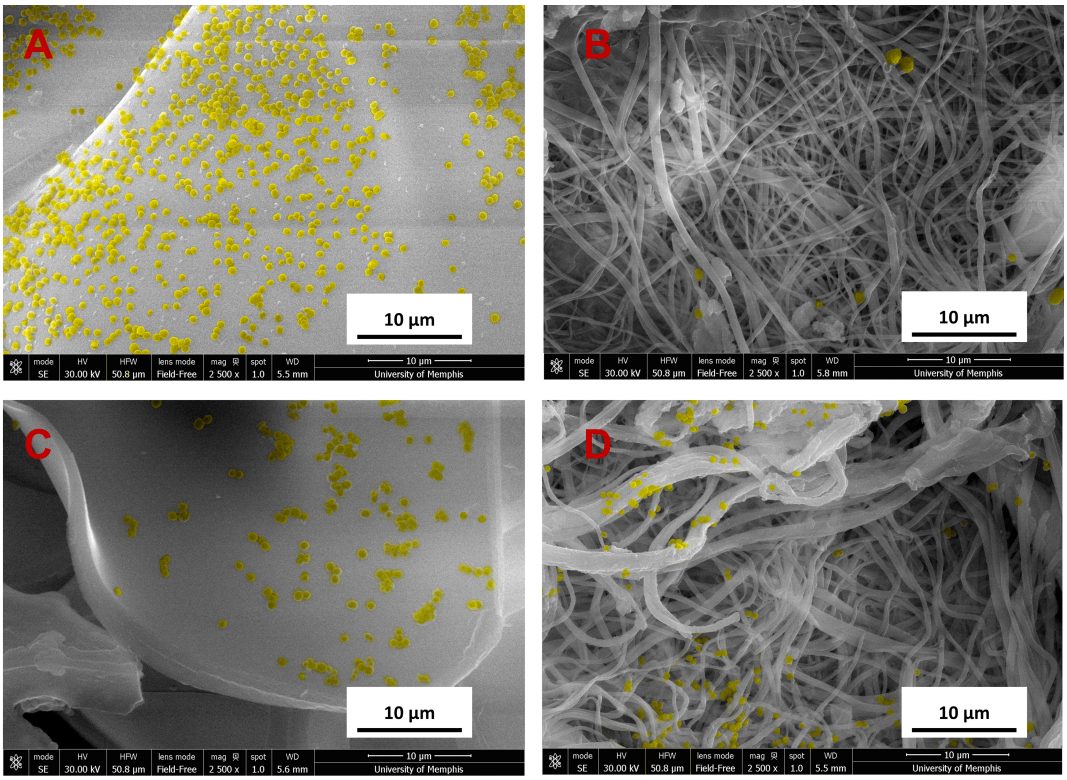

Fig. 9. SEM images of *S. aureus* (yellow) bacteria on samples at 24 hours at 2500× magnification. Letters on images represent (A) Sentrex sponge, (B) DA-treated ESCM, (C) Sentrex sponge loaded with C2DA and Bupivacaine, and (D) DA-treated ESCM loaded with C2DA and Bupivacaine. Images were taken at random with a magnification of 2500× and a spot size of 1. DA, decanoic anhydride.

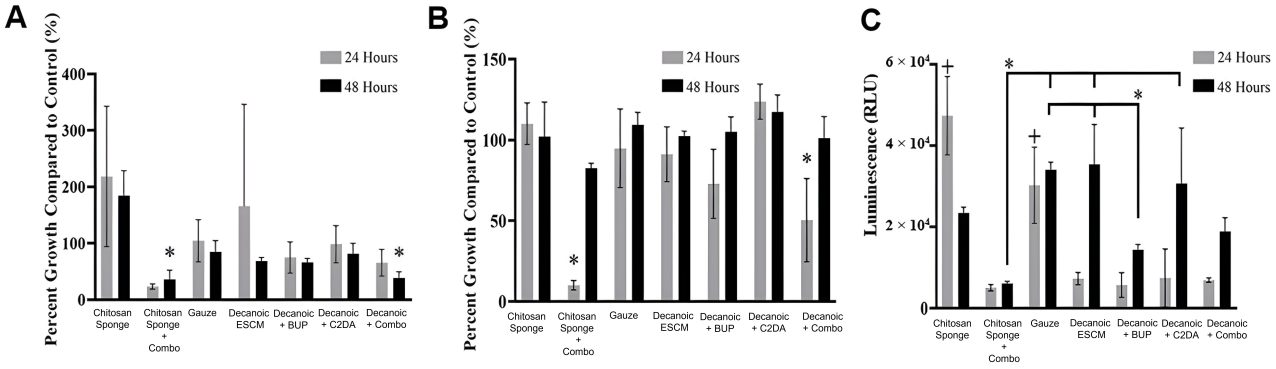

Fig. 10. *A. baumannii* viability at 24 and 48 hours. (A) Planktonic viability, (B) biofilm found in the wells, and (C) biofilm found on samples. Values plotted are the means ± the standard deviation. Significant differences against bacteria control are represented by stars as shown above ($p < 0.05$). Significant differences within groups are represented by asterisks (*) and lines. The plus sign (+) indicates significant difference from all groups. Significant differences were determined by one-way ANOVA, followed by Dunnett C for figures with controls and Kruskal-Wallis ANOVA on ranks, followed by Tukey post-hoc test for figures with no controls (n = 5). BUP, Bupivacaine.

4. Discussion

Overall results of these studies indicate that anhydride modified ESCMs show promising potential to serve as a wound dressing for burn injury applications. Loading ESCMs with therapeutics via ethanol evaporation makes them readily useable in the context of combat-related wounds. Furthermore, local delivery of anesthetics from ESCMs would have the potential to alleviate the unfavorable dependency that follows the use of systemic opioid use and management [18,19] for pain symptoms, while C2DA delivery may prevent infection post-burn. With minimal swelling of anhydride-treated fibers between the experimental groups,

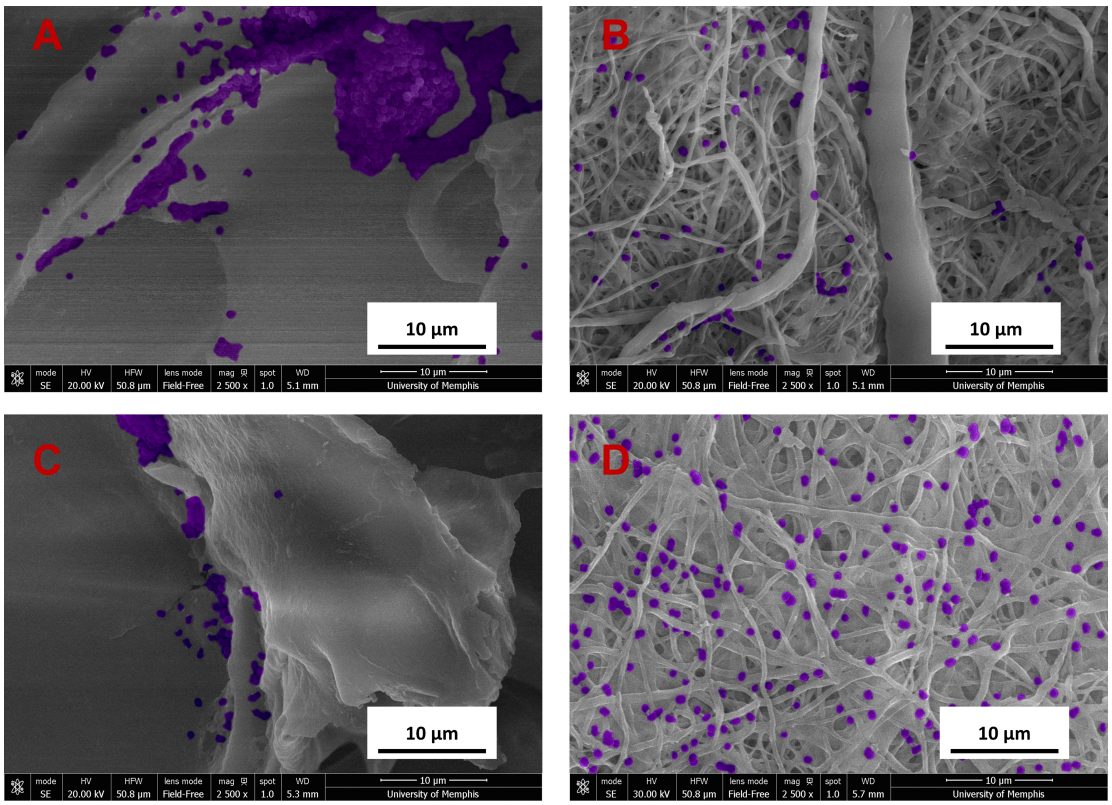

Fig. 11. SEM images of *A. baumannii* (purple) bacteria on samples at 24 hours at 2500× magnification. Letters on images represent (A) Sentrex sponge, (B) DA-treated ESCM, (C) Sentrex sponge loaded with C2DA and Bupivacaine, and (D) DA-treated ESCM loaded with C2DA and Bupivacaine. Images were taken at random with a magnification of 2500× and a spot size of 1.

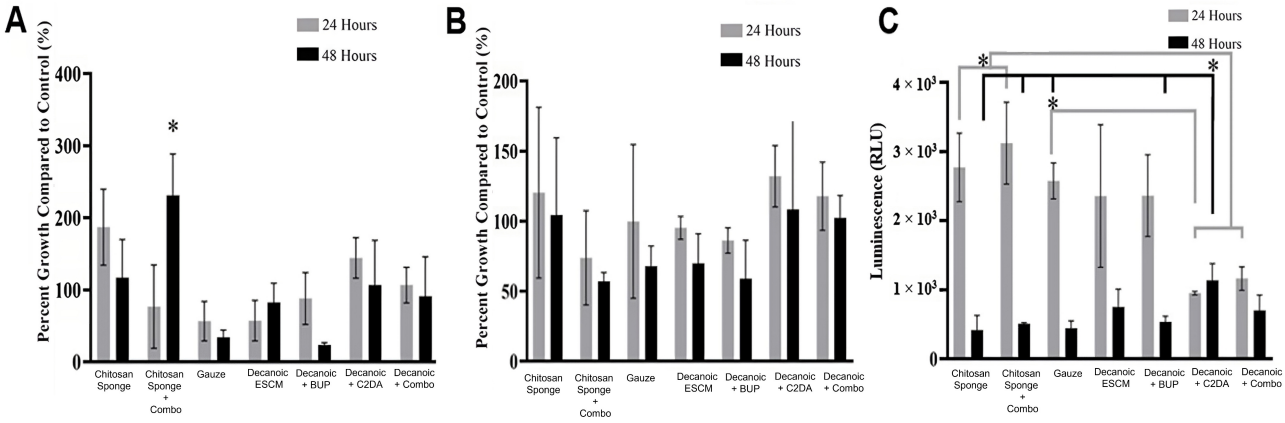

Fig. 12. *P. aeruginosa* viability at 24 and 48 hours. (A) Planktonic viability, (B) biofilm found in the wells, and (C) biofilm found on samples. Values plotted are the means ± the standard deviation. Significant differences against bacteria control are represented by stars as shown above ($p < 0.05$). Significant differences within groups are represented by asterisks (*) and lines. Significant differences were determined by one-way ANOVA, followed by Dunnett C for figures with controls and Kruskal-Wallis ANOVA on ranks, followed by Tukey post-hoc test for figures with no control (n = 5). BUP, Bupivacaine.

we can further tailor ESCMs to be more stable and maintain biological active loading capabilities [32]. Washing ESCMs after treatment successfully removed TFA salts, allowing for a decrease in cytotoxic effects while maintaining hydrophobic properties [24,34]. The DOS calculation showed all of the experimental groups resulting in values less than 2 indicating more viable functional groups available on chitosan, possibly due to steric hindrance making it harder for anhydrides with longer carbon chains to react and bind to chitosan. In return, this allows for the potential loading of more or other therapeutics to further develop this novel burn wound dressing. The degree of substitution

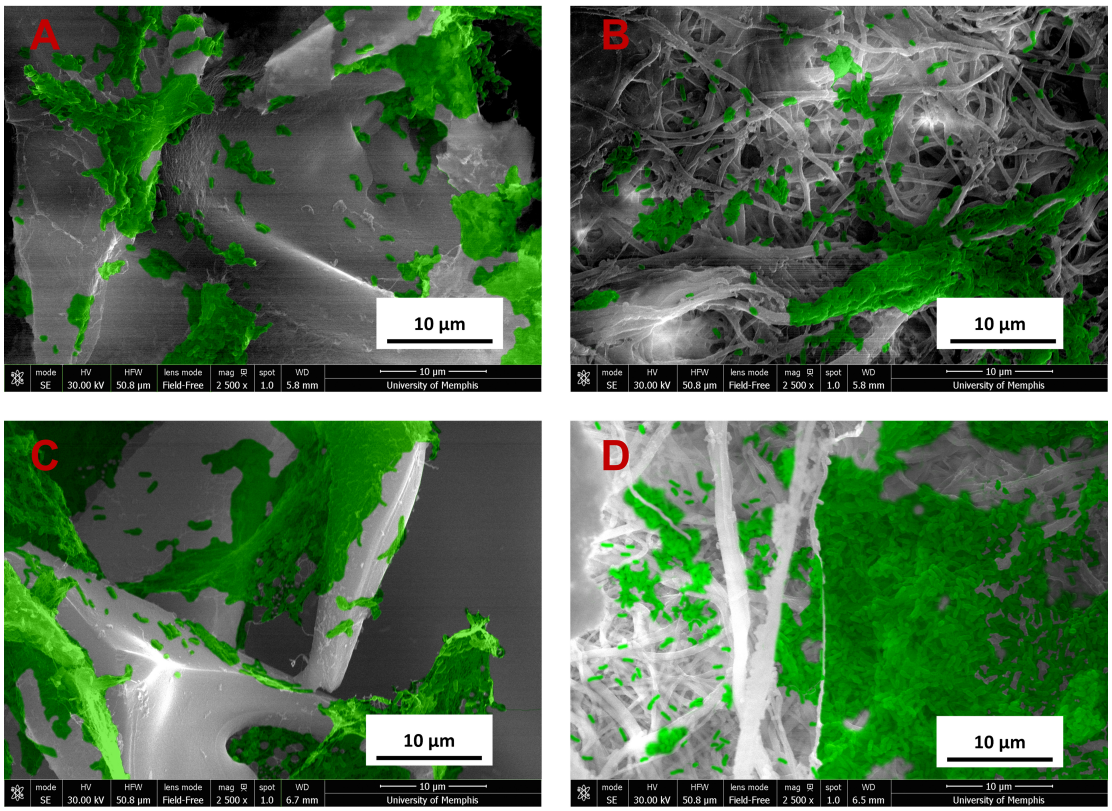

Fig. 13. SEM images of *P. aeruginosa* (green) bacteria on samples at 24 hours at 2500× magnification. Letters on images represent (A) Sentrex sponge, (B) DA-treated ESCM, (C) Sentrex sponge loaded with C2DA and Bupivacaine, and (D) DA-treated ESCM loaded with C2DA and Bupivacaine. Images were taken at random with a magnification of 2500× and a spot size of 1.

indicates how many carbon tails are attached to the electrospun membranes. Therefore, a higher degree of substitution correlates to higher hydrophobicity and larger capacity to encapsulate the drugs loaded. Unlike materials such as the chitosan sponge, the nanofibrous morphology of ESCMs resemble the extracellular matrix with high surface area to volume ratio with pores between the fibers to allow for the excretion of fluids from burn wounds, and reducing the risk of infection [35,36]. Furthermore, it was reported that the electrospun material stimulates extracellular matrix which promotes epithelialization and angiogenesis [36].

Additionally, the intrinsic biofilm inhibitory properties and release of antimicrobial and anti-inflammatory agents may act as a potential burn wound dressing that cuts down on healing time and physiological scarring.

The release of bupivacaine from the dual-loaded experimental ESCMs was similar to another study in which ESCMs treated with hexanoic anhydride (different loading concentrations) resulted in a burst release [25]. Later the study inferred that this burst release is possibly due to excess bupivacaine drying on top of the membranes rather than being loaded in between the acylated fibers [25]. The reduced cumulative release of bupivacaine in control groups compared to experimental suggests that the hydrophobic carbon tails on modified chitosan allow it to capture and hold the hydrophobic drug within the structure. This extended release may provide the patient with pain relief for a longer amount of time and allow for an increase in time between dressing change in dire situations. Although the dual-loaded experimental ESCMs do not release their full payload, for a patient with a compromised immune system, this release may provide a more guided growth not hindered by high concentrations affecting immune/skin cells during the healing process than the release kinetics observed by the control groups.

C2DA release from all groups exhibited a burst release within the first 3 hours, but only the experimental groups eluted through the 24-hour time point suggesting that the hydrophobic interactions from the carbon chains resulted in the drugs being tightly bound within the modified matrix. Furthermore, the absence of C2DA at 12 hours could be attributed to the hydrophobic drugs having low solubility in aqueous environments such as PBS and bovine growth serum as the hydrophilic media outside the hydrophobic nanofibers impedes the diffusion of drugs. These results may be confirmed in future studies using another detection method, such as LC/MS. Our work, though somewhat contrary to similar studies of acylated chitosan membranes, is similar to another local drug delivery system that loaded C2DA onto phosphatidylcholine coatings, resulting in a

burst release at first then tapering concentrations afterward [15]. The cumulative release of C2DA in all groups was less than the total loaded amount, suggesting that the samples are holding onto C2DA more tightly, possibly due to the chain length and configuration of the anhydride treatment on the hydroxyl group of chitosan allowing for attachment of long carbon chains dictating its time-dependent release. The long-tail carbon chains associate with the hydrophobic portions of the loaded drugs. Hydrophobic molecules aggregate in aqueous environments which restricts their contact with water and encapsulates the hydrophobic molecules within the chitosan matrix [37]. The retention of the drugs inside the matrix allows for a slower, controlled release as the drugs have to overcome the strong hydrophobic interactions to diffuse out [24].

Future studies will be performed to measure the C2DA within the samples more accurately via HPLC detection after chemically/physically destroying the samples for detecting therapeutics that may reside within the fibers. Additionally, although not fully understood, the synergistic effect [14] from loading C2DA with bupivacaine may play a role in release kinetics.

Activity against strains prevalent in burn injuries suggests these biomaterials would be useful in burn injury infection prevention. Similar antimicrobial activity against *S. aureus* was reported in a study performed by Harrison *et al*. [25], where the same therapeutics and method of delivery were used, but at much higher concentrations. In this study, nearly all groups had decreased growth within 24 hours, even groups not loaded with any therapeutic [25], indicating that materials themselves were inhibitory to bacteria, but not bactericidal at these concentrations. In contrast, our study looked at the response by 48 hours, where the only biomaterials with significant antibacterial properties were those loaded with both therapeutics, which suggests that the combination of therapeutics may have additive or synergistic effects for inhibition of biofilm. The absence of differences between the modified chitosan and control groups against planktonic *A baumannii* may be due to the lower susceptibility of this strain to both bupivacaine and C2DA. This is further confirmed by the reduced growth of planktonic bacteria at 48 hours only in the groups that received both drugs. The reduction however was not observed in *P. aeruginosa* planktonic data suggesting that the combination and concentration of both therapeutics seems to be more effective at inhibiting *S. aureus* and *A. baumannii* planktonic bacteria compared with planktonic *P. aeruginosa*. The decreased efficacy of the drugs is likely due to *P. aeruginosa* being one of the gram-negative strains that become harder to treat as time increases in comparison with other skin related infections from burn wounds [38]. Reports of high concentrations of C2DA have found that this agent increases cell membrane permeability [39], and *P. aeruginosa* among other strains produce and utilize these DSFs [12], which would explain the lack of inhibition of *P. aeruginosa* at such concentrations compared to that of other strains. It is likely that the antimicrobial activity exhibited by gauze is due to the processing method of the gauze, as they are bleached for color and sterility purposes. The lack of an inhibitory effect against the gram-negative strains may also be explained by the burst release seen in the elution studies, where a burst release of C2DA is followed by tapering concentration within the first day. The reduction of *S. aureus* and *P. aeruginosa*'s biofilm in the wells, below the samples, at 48 hours may be due to the increase in time resulting in more available therapeutics in the wells. In addition to more therapeutics being released, it is also important to note that most of these samples are hydrophobic and float within the TSB media, resulting in an increase of therapeutics reaching the bottoms of the wells via diffusion over time. The higher growth of *S. aureus* and *A. baumannii* biofilm on the chitosan sponge suggests that the material alone was not able to reduce the viability of biofilm for both time points as opposed to the experimental groups such as the decanoic anhydride modified ESCM, indicating it may have an inhibitory effect on its own. Groups loaded with both therapeutics reduced *P. aeruginosa* biofilm growth at 48 hours, which suggests that Bupivacaine and C2DA might have an additive effect on some strains of bacteria.

Future studies for this project entail a reconsideration of loading concentrations, *in vivo* studies, and exploring different loading strategies. Additional future studies include cytocompatibility studies using human dermal fibroblasts and keratinocytes. Other synthetic analogs of C2DA have been developed as well as new procedures for measuring therapeutics, so future studies may include incorporation of these analogs into chitosan membranes and evaluation of their potential to prevent and eradicate biofilm more effectively than C2DA. Although ESCMs loaded with C2DA and bupivacaine seem promising, there are still limitations; the antimicrobial efficacy of ESCMs modified with different chain lengths and the effects of different treatment methods on the DOS were not explored. Furthermore, different loading strategies to increase drug encapsulation capacity, and i*n vivo* studies are needed to evaluate how the use of ESCMs as wound dressings could be translated to clinical use.

5. Conclusions

These *in vitro* evaluations investigated combination and individual loading of therapeutics for control and experimental groups to aid in pain relief and infection prevention as a burn wound dressing application. In austere locations or combat settings, where medical attention may be delayed, an antibacterial wound dressing may be advantageous for minimizing infections from further contamination as well as potential biofilm growth within the first 24 hours of administration, with local anesthetics remaining active over the course of 72 hours, until further care is available. Extending the alkyl chain length in modified

ESCMs by using anhydrides with longer chains such as decanoic anhydride could increase hydrophobicity, promote better biocompatibility, and improve chemical and mechanical stability. Longer carbon chains also facilitate sustained drug release since they provide a diffusion barrier. Based on findings from the bacterial studies it is suggested that the combination of therapeutics play a major role in biofilm prevention for select strains such as *S. aureus*, *A. baumannii*, and *P. aeruginosa*, whether that is from direct contact or diffusion in aqueous solutions. To conclude, this *in vitro* study denotes the potential of varying acylated ESCMs, especially decanoic-modified, to be used as a burn wound dressing by releasing hydrophobic therapeutics for prevention of bacterial/biofilm growth and pain relief.

Availability of Data and Materials

The data are available from the corresponding author upon request.

Author Contributions

Research idea and study design, JDB, LRC and JAJ; bacterial growth and membrane treatments, LRC, ZH, EA, and ECM; data analysis and interpretation, TF, LRC, ZH, ECM, EA and JRB; supervision, JAJ, TF, JDB. All authors have been involved in drafting and revising the manuscript, and all authors have been involved in revising it critically for important intellectual content. All authors read and approved the final manuscript. All authors have participated sufficiently in the work and agreed to be accountable for all aspects of the work.

Ethics Approval and Consent to Participate

Not applicable.

Acknowledgment

We thank Ashleigh Anderson, Alex Bryan, Brenna Ballard, Claire Abrey, and Bharat Jothlingham for assistance in membrane fabrication, imaging, sampling, and text editing.

Funding

Research is supported by the Military Burn Research Program (MBRP) under Award #: W81XWH-20-1-0430 and the University of Memphis/University of Tennessee Health Science Center Joint Program in Biomedical Engineering.

Conflict of Interest

Given the role of Dr. Jessica Amber Jennings, and Dr. Josh Bush as Guest editors of Special Issue, they had no involvement in the peer-review of this article and have no access to information regarding its peer review. Full responsibility for the editorial process for this article was delegated to Viviana di Giacomo and Piergiorgio Gentile. The authors declare no conflict of interest.

References

[1] World Health Organization. Burns Fact Sheet. 2023. Available at: https://www.who.int/news-room/fact-sheets/detail/burns (Accessed: 3 January 2024).

[2] Jeschke MG, van Baar ME, Choudhry MA, Chung KK, Gibran NS, Logsetty S. Burn injury. Nature Reviews. Disease Primers. 2020; 6: 11.

[3] Davis SC, Ricotti C, Cazzaniga A, Welsh E, Eaglstein WH, Mertz PM. Microscopic and physiologic evidence for biofilm-associated wound colonization in vivo. Wound Repair and Regeneration. 2008; 16: 23–29.

[4] Sudhan S S, Sharma P, Sharma K, Sharma M, Sambyal SS. Time Related Emergence of Bacterial Pathogens and their Antibiograms in Burn Wound Infections in a Tertiary Care Hospital. International Journal of Current Microbiology and Applied Sciences. 2017; 6: 416–422.

[5] Römling U, Balsalobre C. Biofilm infections, their resilience to therapy and innovative treatment strategies. Journal of Internal Medicine. 2012; 272: 541–561.

[6] Lewis K. Persister cells. Annual Review of Microbiology. 2010; 64: 357–372.

[7] Hoffmann S. Silver sulfadiazine: an antibacterial agent for topical use in burns. A review of the literature. Scandinavian Journal of Plastic and Reconstructive Surgery. 1984; 18: 119–126.

[8] Cancio LC, Barillo DJ, Kearns RD, Holmes JH, 4th, Conlon KM, Matherly AF, *et al*. Guidelines for Burn Care Under Austere Conditions: Surgical and Nonsurgical Wound Management. Journal of Burn Care & Research. 2017; 38: 203–214.

[9] Khansa I, Schoenbrunner AR, Kraft CT, Janis JE. Silver in Wound Care-Friend or Foe?: A Comprehensive Review. Plastic and Reconstructive Surgery. Global Open. 2019; 7: e2390.

[10] Deng Y, Lim A, Lee J, Chen S, An S, Dong YH, *et al*. Diffusible signal factor (DSF) quorum sensing signal and structurally related molecules enhance the antimicrobial efficacy of antibiotics against some bacterial pathogens. BMC Microbiology. 2014; 14: 51.

[11] Solano C, Echeverz M, Lasa I. Biofilm dispersion and quorum sensing. Current Opinion in Microbiology. 2014; 18: 96–104.

[12] Davies DG, Marques CNH. A fatty acid messenger is responsible for inducing dispersion in microbial biofilms. Journal of Bacteriology. 2009; 191: 1393–1403.

[13] Abraham WR. Going beyond the Control of Quorum-Sensing to Combat Biofilm Infections. Antibiotics. 2016; 5: 3.

[14] Masters E, Harris M, Jennings J. Cis-2-decenoic acid interacts with bacterial cell membranes to potentiate additive and synergistic responses against biofilm. Journal of Bacteriology and Mycology. 2016; 3: 1–8.

[15] Harris MA, Beenken KE, Smeltzer MS, Haggard WO, Jennings JA. Phosphatidylcholine Coatings Deliver Local Antimicrobials and Reduce Infection in a Murine Model: A Preliminary Study. Clinical Orthopaedics and Related Research. 2017; 475: 1847–1853.

[16] Dissanaike S, McCauley J, Alphonso C. Liposomal bupivacaine for the management of postsurgical donor site pain in patients with burn injuries: a case series from two institutions. Clinical Case Reports. 2017; 6: 129–135.

[17] Jönsson A, Brofeldt BT, Nellgård P, Tarnow P, Cassuto J. Local anesthetics improve dermal perfusion after burn injury. The Journal of Burn Care & Rehabilitation. 1998; 19: 50–56.

[18] Hollmann MW, Durieux ME. Local anesthetics and the inflammatory response: a new therapeutic indication? Anesthesiology. 2000; 93: 858–875.

[19] Razavi BM, Fazly Bazzaz BS. A review and new insights to antimicrobial action of local anesthetics. European Journal of Clinical Microbiology & Infectious Diseases. 2019; 38: 991–1002.

[20] Younes I, Rinaudo M. Chitin and chitosan preparation from marine sources. Structure, properties and applications. Marine Drugs. 2015; 13: 1133–1174.
[21] Parker AC, Jennings JA, Bumgardner JD, Courtney HS, Lindner E, Haggard WO. Preliminary investigation of crosslinked chitosan sponges for tailorable drug delivery and infection control. Journal of Biomedical Materials Research. Part B, Applied Biomaterials. 2013; 101: 110–123.
[22] Harris M, Ahmed H, Barr B, LeVine D, Pace L, Mohapatra A, *et al*. Magnetic stimuli-responsive chitosan-based drug delivery biocomposite for multiple triggered release. International Journal of Biological Macromolecules. 2017; 104: 1407–1414.
[23] Pace LR, Harrison ZL, Brown MN, Haggard WO, Jennings JA. Characterization and Antibiofilm Activity of Mannitol-Chitosan-Blended Paste for Local Antibiotic Delivery System. Marine Drugs. 2019; 17: 517.
[24] Murali VP, Fujiwara T, Gallop C, Wang Y, Wilson JA, Atwill MT, *et al*. Modified electrospun chitosan membranes for controlled release of simvastatin. International Journal of Pharmaceutics. 2020; 584: 119438.
[25] Harrison ZL, Bumgardner JD, Fujiwara T, Baker DL, Jennings JA. In vitro evaluation of loaded chitosan membranes for pain relief and infection prevention. Journal of Biomedical Materials Research. Part B, Applied Biomaterials. 2021; 109: 1735–1743.
[26] Bhattarai N, Edmondson D, Veiseh O, Matsen FA, Zhang M. Electrospun chitosan-based nanofibers and their cellular compatibility. Biomaterials. 2005; 26: 6176–6184.
[27] Noel SP, Courtney H, Bumgardner JD, Haggard WO. Chitosan films: a potential local drug delivery system for antibiotics. Clinical Orthopaedics and Related Research. 2008; 466: 1377–1382.
[28] Chen ZG, Wang PW, Wei B, Mo XM, Cui FZ. Electrospun collagen-chitosan nanofiber: a biomimetic extracellular matrix for endothelial cell and smooth muscle cell. Acta Biomaterialia. 2010; 6: 372–382.
[29] Jayakumar R, Prabaharan M, Nair SV, Tamura H. Novel chitin and chitosan nanofibers in biomedical applications. Biotechnology Advances. 2010; 28: 142–150.
[30] Mendes AC, Gorzelanny C, Halter N, Schneider SW, Chronakis IS. Hybrid electrospun chitosan-phospholipids nanofibers for transdermal drug delivery. International Journal of Pharmaceutics. 2016; 510: 48–56.
[31] Cofsky R, Vangala K, Haag R, Recco R, Maccario E, Sathe S, *et al*. The cost of antibiotic resistance: effect of resistance among Staphylococcus aureus, Klebsiella pneumoniae, Acinetobacter baumannii, and Pseudmonas aeruginosa on length of hospital stay. Infection Control and Hospital Epidemiology. 2002; 23: 106–108.
[32] Wu C, Su H, Tang S, Bumgardner JD. The stabilization of electrospun chitosan nanofibers by reversible acylation. Cellulose. 2014; 21: 2549–2556.
[33] Bayat S, Amiri N, Pishavar E, Kalalinia F, Movaffagh J, Hashemi M. Bromelain-loaded chitosan nanofibers prepared by electrospinning method for burn wound healing in animal models. Life Sciences. 2019; 229: 57–66.
[34] Murali VP, Guerra FD, Ghadri N, Christian JM, Stein SH, Jennings JA, *et al*. Simvastatin loaded chitosan guided bone regeneration membranes stimulate bone healing. Journal of Periodontal Research. 2021; 56: 877–884.
[35] Azimi B, Maleki H, Zavagna L, De la Ossa JG, Linari S, Lazzeri A, *et al*. Bio-Based Electrospun Fibers for Wound Healing. Journal of Functional Biomaterials. 2020; 11: 67.
[36] Ketabchi N, Dinarvand R, Adabi M, Gholami M, Firoozi S, Amanzadi B, *et al*. Study of third-degree burn wounds debridement and treatment by actinidin enzyme immobilized on electrospun chitosan/PEO nanofibers in rats. Biointerface Research in Applied Chemistry. 2021; 11: 10358–10370.
[37] Philippova OE, Korchagina EV. Chitosan and its hydrophobic derivatives: Preparation and aggregation in dilute aqueous solutions. Polymer Science Series A. 2012; 54: 552–572.
[38] Lachiewicz AM, Hauck CG, Weber DJ, Cairns BA, van Duin D. Bacterial Infections After Burn Injuries: Impact of Multidrug Resistance. Clinical Infectious Diseases. 2017; 65: 2130–2136.
[39] Jennings JA, Courtney HS, Haggard WO. Cis-2-decenoic acid inhibits S. aureus growth and biofilm in vitro: a pilot study. Clinical Orthopaedics and Related Research. 2012; 470: 2663–2670.